

NONLINEAR OPTICAL PHENOMENA

PACS numbers: 42.25.Ls; 42.50.Gy
DOI: 10.1070/QE2015v045n11ABEH015822

Transient birefringence effects in electromagnetically induced transparency

O.M. Parshkov

Abstract. **We report the results of numerical modelling of transient birefringence that arises as a result of electromagnetically induced transparency on degenerate quantum transitions between the states with $J = 0$, 1 and 2 in the presence of the Doppler broadening of spectral lines. It is shown that in the case of a linearly polarised control field, the effect of transient birefringence leads to a decay of the input circularly polarised probe pulse into separate linearly polarised pulses inside a medium. In the case of a circularly polarised control field, the effect of transient birefringence manifests itself in a decay of the input linearly polarised probe pulse into separate circularly polarised pulses. It is shown that the distance that a probe pulse has to pass in a medium before decaying into subpulses is considerably greater in the first case than in the second. The influence of the input probe pulse power and duration on the process of spatial separation into individual pulses inside a medium is studied. A qualitative analysis of the obtained results is presented.**

Keywords: *electromagnetically induced transparency, transient effects, birefringence.*

1. Introduction

Investigation of electromagnetically induced transparency (EIT) [1] is of great importance both from a theoretical and applied perspective. It has led to a significant progress in optical quantum-memory systems [2], quantum communications [2–4], quantum information theory [1, 2, 5], high-precision magnetometry [6], atomic frequency standards [7], creation of large optical nonlinearities [5, 8] and radiation amplification without population inversion [9, 10]. To date, the range of media, in which the EIT phenomenon is observed, is quite wide. It includes not only atomic and molecular gases but also solids with rare-earth impurities [11], semiconductor quantum wells [12], superconducting structures [13] and metamaterials [14].

At the initial stage of the EIT theory development, the interaction of radiations was modelled on the basis of Λ-, V- and Ξ-type schemes of quantum transitions [5] formed by simple energy levels. Complication of the schemes of these transitions by increasing the number of fields and simple energy levels has led to theoretical and experimental discovery of a number of specific manifestations of EIT in more complex schemes of nondegenerate transitions [9, 15–17].

Investigation of EIT on degenerate quantum transitions opened new features of this phenomenon, among which an important place is occupied by the effects of changes in the polarisation state of interacting fields. For example, the authors of Refs [18, 19] studied theoretically and experimentally the rotation of the polarisation plane of a probe field by changing the control field intensity. In Refs [20, 21], the effect of a constant magnetic field on the process of evolution of circular components of probe laser light was theoretically and experimentally investigated under conditions of EIT. Linear and circular birefringence of a probe field in EIT was studied theoretically and experimentally in [22]. In theoretical work [23] the authors predicted the possibility of probe field propagation as a result of EIT in the form of two modes with different polarisation states.

In the above papers, the authors considered a stationary (steady) wave interaction regime, which corresponds to a situation when the durations of both light pulses participating in EIT far exceed the irreversible relaxation times of quantum transitions. In this case, the time dependence of the radiation intensity and population level can be neglected. The opposite situation, which we call a transient EIT regime, occurs when the pulse duration of at least one of the interacting fields is less than the irreversible relaxation times or comparable with them. This regime is more promising in terms of practical applications of the EIT phenomenon in quantum communication and information systems [1, 2, 4, 5]. In [24, 25] we have shown that EIT on degenerate quantum transitions in the transient regime leads to a decay of the input linearly polarised probe pulse into several subpulses that are circularly polarised in opposite directions, in the case if the input pulse of the control field is circularly polarised.

This paper presents the results of numerical modelling of the EIT effect on polarisation characteristics of the probe field in the transient regime. It is shown that this influence can lead to the splitting of a circularly polarised input probe pulse into a set of linearly polarised pulses. In addition, the characteristics of this process are compared with the characteristics of the process described in [24, 25]. The results are interpreted as a specific manifestation of birefringence that accompanies EIT.

Our approach takes into account the inhomogeneous broadening of quantum transition lines and is not limited by the weak probe field approximation typically used in the analysis of the EIT impact on the evolution of the polarisation states of light. Calculations have been carried out for the quantum transitions between degenerate energy levels $^3P_0$, $^3P_2$

O.M. Parshkov Yuri Gagarin State Technical University of Saratov, ul. Politekhnicheskaya 77, 410054 Saratov, Russia;
e-mail: oparshkov@mail.ru

Received 1 April 1 2015
Kvantovaya Elektronika **45** (11) 1010–1017 (2015)
Translated by I.A. Ulitkin

and $^3P_1^0$ of the ^{208}Pb isotope, in whose vapours EIT of circularly polarised laser fields was observed [26].

2. Statement of the problem

Consider a lambda scheme consisting of the nondegenerate ($J = 0$) lower, five-fold degenerate ($J = 2$) middle and triply degenerate ($J = 1$) upper levels. This scheme is formed, for example, by levels $^3P_0$, $^3P_2$ and $^3P_1^0$ of ^{208}Pb isotope or ^{118}Sn and ^{120}Sn isotopes. Let ϕ_k ($k = 1, 2, \ldots, 9$) be the orthonormalised basis of common eigenfunctions of the operators of energy, square and z component of the momentum for an isolated atom, which correspond to the lower ($k = 1$, $M = 0$), upper ($k = 2, 3, 4$, $M = -1, 0, 1$) and middle ($k = 5, 6, \ldots, 9$, $M = -2, -1, 0, 1, 2$) levels. Let D_1 and D_2 be reduced electric dipole moments for the $J = 0 \to J = 1$ and $J = 2 \to J = 1$ transitions, respectively, and ω_1 and ω_2 ($\omega_1 > \omega_2$) be the frequencies of these transitions for an atom at rest. We also set $T_1 = 1/\Delta_1$, where Δ_1 is the Doppler half-width (at the e^{-1} level) of the density distribution of the quantum transition ($J = 0 \to J = 1$) frequencies ω_1'.

We represent the electric field of two laser pulses propagating along the z axis with carrier frequencies ω_1 and ω_2 (probe and control pulses, respectively; $\omega_1 > \omega_2$) in the form

$$\boldsymbol{E} = \mathrm{Re}\sum_{l=1}^{2}\mu_l(\boldsymbol{e}_+ f_l + \boldsymbol{e}_- g_l)\exp[\mathrm{i}(\omega_l t - k_l z)], \tag{1}$$

where $\mu_l = \hbar\sqrt{2l+1}/(|D_1|T_1)$; $\boldsymbol{e}_+ = \boldsymbol{e}_-^* = (\boldsymbol{i} + \mathrm{i}\boldsymbol{j})/2$; $\boldsymbol{i}$ and $\boldsymbol{j}$ are the unit vectors of the x and y axes; f_l and g_l are the complex amplitudes of the right- (σ_-) and left-hand (σ_+) circular components [27] of the probe ($l = 1$) and control ($l = 2$) fields, which are functions of z and t; and $k_l = \omega_l/c$.

We represent the wave function of the atom in the form

$$\Psi = \bar{c}_1\phi_1 + \left(\sum_{k=2}^{4}\bar{c}_k\phi_k\right)\exp(-\mathrm{i}\xi_1) + \left(\sum_{k=5}^{9}\bar{c}_k\phi_k\right)\exp[-\mathrm{i}(\xi_1 - \xi_2)], \tag{2}$$

where $\xi_l = \omega_l t - k_l z$, and introduce the quantities

$$c_1 = p_1^*\bar{c}_1, \quad c_2 = \bar{c}_2, \quad c_4 = \bar{c}_4, \quad c_5 = p_2\bar{c}_5,$$

$$c_7 = (1/\sqrt{6})p_2\bar{c}_7, \quad c_9 = p_2\bar{c}_9,$$

where $p_l = 2D_l/|D_l|$. We define the normalised independent variables s and w as

$$s = z/z_0, \quad w = (t - z/c)/T_1, \tag{3}$$

where $z_0 = 3\hbar c/(2\pi N|D_1|^2 T_1\omega_1)$ and N is the concentration of atoms. By using the Maxwell and Schrödinger equations and (1) and (3) we obtain, in the slowly varying amplitude approximation, the system of equations:

$$\begin{aligned}
&\frac{\partial f_1}{\partial s} = \frac{\mathrm{i}}{\sqrt{\pi}}\int_{-\infty}^{+\infty} c_1 c_2^*\exp(-\varepsilon_1^2)\,\mathrm{d}\varepsilon_1,\\
&\frac{\partial f_2}{\partial s} = -\frac{\mathrm{i}}{\sqrt{\pi}}\xi\int_{-\infty}^{+\infty}(c_4^* c_9 + c_2^* c_7)\exp(-\varepsilon_1^2)\,\mathrm{d}\varepsilon_1,\\
&\frac{\partial g_1}{\partial s} = -\frac{\mathrm{i}}{\sqrt{\pi}}\int_{-\infty}^{+\infty} c_1 c_4^*\exp(-\varepsilon_1^2)\,\mathrm{d}\varepsilon_1,\\
&\frac{\partial g_2}{\partial s} = \frac{\mathrm{i}}{\sqrt{\pi}}\xi\int_{-\infty}^{+\infty}(c_2^* c_5 + c_4^* c_7)\exp(-\varepsilon_1^2)\,\mathrm{d}\varepsilon_1,\\
&\frac{\partial c_1}{\partial w} = -\mathrm{i}(f_1 c_2 - g_1 c_4),\\
&\frac{\partial c_2}{\partial w} + \mathrm{i}\varepsilon_1 c_2 = -\frac{\mathrm{i}}{4}(f_1^* c_1 + g_2^* c_5 - f_2^* c_7) - \gamma c_2,\\
&\frac{\partial c_4}{\partial w} + \mathrm{i}\varepsilon_1 c_4 = \frac{\mathrm{i}}{4}(g_1^* c_1 - g_2^* c_7 + f_2^* c_9) - \gamma c_4,\\
&\frac{\partial c_5}{\partial w} + \mathrm{i}(\varepsilon_1 - \varepsilon_2)c_5 = -\mathrm{i}g_2 c_2,\\
&\frac{\partial c_7}{\partial w} + \mathrm{i}(\varepsilon_1 - \varepsilon_2)c_7 = \frac{\mathrm{i}}{6}(f_2 c_2 - g_2 c_4),\\
&\frac{\partial c_9}{\partial w} + \mathrm{i}(\varepsilon_1 - \varepsilon_2)c_9 = -\mathrm{i}f_2 c_4,
\end{aligned} \tag{4}$$

where

$$\varepsilon_1 = \frac{\omega_1' - \omega_1}{\Delta_1}; \quad \varepsilon_2 = \frac{\omega_2}{\omega_1}\varepsilon_1; \quad \xi = 0.75\frac{\omega_2}{\omega_1}\left|\frac{D_2}{D_1}\right|^2. \tag{5}$$

In accordance with the selection rules ($\Delta M = \pm 1$) for transitions affected by the circular components of the field (1), the amplitudes $\bar{c}_3$, $\bar{c}_6$ and $\bar{c}_8$ are not included in (4). Taking into account the Doppler broadening of quantum transition lines by averaging the field-induced dipole moments of individual atoms with respect to the parameter ε_1 that is uniquely associated with the velocity of the thermal motion of each atom along the z axis has led to the emergence of integrals in the first four equations of system (4) and to a specific coupling between the quantities ε_1 and ε_2. In equations for c_2 and c_4, we have phenomenologically introduced the terms $-\gamma c_2$ and $-\gamma c_4$ to account for the spontaneous decay of the upper level states of the lambda scheme in question. The quantity $\gamma = T_1/(2\tau)$, where τ is the radiative lifetime of the $6p7s\,^3P_1^0$ level.

The presence of partial time derivatives w in the equations of system (4) results in a delay of the polarisation response of a medium to the action of the fields. If the delay significantly affects the evolution of the waves, then the regime of their interaction with the medium is called transient. This regime is usually implemented in cases when the effect of radiation on the medium has a duration comparable to or much less than the irreversible relaxation times of quantum transitions.

To describe the polarisation states of radiation we use the parameters a_l, α_l, γ_l of the polarisation ellipses of probe ($l = 1$) and control ($l = 2$) fields. Here, a_l is the semi-major axis of the ellipse, measured in μ_l units; α_l is the angle of its inclination to the x axis; and γ_l is the quantity of contraction ($a_l \geqslant 0$, $0 \leqslant \alpha_l < \pi$, $|\gamma_l| \leqslant 1$ [27]). The quantity $|\gamma_l|$ determines the ratio of the minor axis of the ellipse to its major axis. The condition $0 < \gamma_l < 1$ ($-1 < \gamma_l < 0$) corresponds to the right-hand (left-hand) elliptical polarisation, and the condition $\gamma_l = 0$ – to the linear polarisation; at $\gamma_l = 1$ the polarisation is right-handed circular (σ_- polarisation), whereas at $\gamma_l = -1$ the polarisation is left-handed circular (σ_+ polarisation). When $|\gamma_l| = 1$, the angle a_l is not defined and, in our calculations, we formally set it equal to -0.1.

Boundary conditions describing the probe field at the input surface, $s = 0$, have been selected in the form

$$\alpha_1 = \alpha_{10}, \quad a_1 = a_{10}\mathrm{sech}[(w - w_0)/\tau_1], \quad \gamma_1 = \gamma_{10}, \tag{6}$$

and the control field was given by the relation

$$\alpha_2 = \alpha_{20}, \quad a_2 = a_{20}, \quad \gamma_2 = \gamma_{20}, \tag{7}$$

where α_{l0}, a_{l0}, γ_{l0} are some constants. It was assumed that before the arrival of the probe pulse ($w \leqslant 0$) only the lower energy level is populated.

Equalities (6) describe an input bell-like probe pulse of duration $1.76\tau_1$ (at the half of the peak intensity) in units of time w. The top of this pulse intersects the input surface at an instant of time w_0. Equations (7) describe the input control field whose intensity does not vary during the entire process of the wave interaction.

Calculations were carried out for the lambda scheme formed by levels $^3P_0$, $^3P_2$ and $^3P_1^0$ of isotope ^{208}Pb. According to [28], for the selected transitions in ^{208}Pb, in formulas (4) and (5) we use $\omega_2/\omega_1 = 0.7$, $\xi = 2.11$ and (if $T = 900-1000$ K) $\gamma = 1.5 \times 10^{-2}$. When $T = 950$ K, we have $T_1 = 1.63 \times 10^{-10}$ s. Selecting the saturated ^{208}Pb vapours for the estimates and using the data of [29], we obtain $N = 3.4 \times 10^{13}$ cm^{-3} and $z_0 = 0.03$ cm at the same temperature. Note that z_0 is the distance, at which, due to the presence of an inhomogeneous broadening, the intensity of a weak probe pulse decreases by about a factor of e in the absence of the control field. The quantity z_0 strongly depends on temperature. Thus, $z_0 =$ 0.1 and 0.01 cm at $T = 900$ and 1000 K, respectively. The time T_1 is weakly dependent on temperature and decreases by about 5% at such a variation. The quantities z_0 and T_1 are the normalising factors in a transition from independent variables z, t to dimensionless variables s, w by formulas (3). The time τ of the radiative decay of the $^3P_1^0$ level, playing the role of the irreversible relaxation time of a quantum system at a low vapour density, is about 6 ns [28].

To present the results of calculations we use the dimensionless intensities I_l, i.e., energy flux densities of the probe ($l = 1$) and control ($l = 2$) fields, measured in $c\mu_1^2/(8\pi)$ units. Dimensional intensities $\bar{I}_l$ (kW cm^{-2}) of the probe and control fields in the temperature range of 900–1000 K can be estimated as $\bar{I}_l = 1.3I_l$. The transmittance T_m characterises the transparency of a medium for the probe field and is determined by the formula $T_m = W_1(s)/W_1(0)$, where $W_1(0)$ and $W_1(s)$ are the energies (calculated per unit sectional area) of the probe pulse at the input to a resonant medium and at a distance s in the medium, respectively.

The main attention in our work is focused on the situation where the pulse of the input probe field has the σ_+ polarisation ($\gamma_{10} = -1$), whereas the input control field is linearly polarised ($\gamma_{20} = 0$). This EIT regime we hereafter call regime I. Regime II is the one that corresponds to the situation described in [24, 25], when the input probe field is linearly polarised ($\gamma_{10} = 0$) and the input control field is circularly polarised ($\gamma_{20} = -1$). Regime III corresponds to the case of collinear linear polarisations of the input pulse ($\alpha_{10} = \alpha_{20}$, $\gamma_{10} = \gamma_{20} = 0$). This regime for the lambda scheme in question can be described by EIT theory on degenerate quantum transitions. To compare the results of calculations the parameters a_{10}, a_{20} and τ_1 are chosen such that the peak intensities and durations of input probe pulses coincide and the intensities of the control fields are identical ($I_2 = 16$). For each regime we study the cases of strong and weak input probe pulses, whose peak intensities are equal to 1/4 and 1/320 of the intensity of the input control field, respectively. We also present the results of calculations in regime I for a strong input probe pulse with a duration that is ten times greater than the duration of input probe pulses in previous calculations.

3. Results of calculations

1. Consider EIT in regime I for a strong input probe pulse. To do this, we set $\tau_1 = 5$, $\alpha_{10} = -0.1$ rad, $a_{20} = \sqrt{2}$, $\gamma_{10} = -1$, $\alpha_{20} =$ 0.5 rad, $a_{20} = 7.0$ and $\gamma_{20} = 0$ in (6) and (7). Note that the chosen value of τ_1 corresponds to a dimensional probe-pulse duration of 1.5 ns (at $T = 950$ K), while the irreversible relaxation time τ is 6 ns. Continuous curves in Fig. 1 show the results of calculations of the dependences of the probe and control field intensities on w for several fixed distances s. Dashed curves show the dependences of the probe pulse intensity in regime III. In this case, these curves represent a probe component of a (known in EIT theory) pulsed pair that is called an adiabaton [30].

According to Fig. 1, the input probe pulse decays into two pulses in a medium. The first one (pulse 1 in Figs 1c, d) propagates in a medium at a velocity of the adiabaton probe pulse, while the velocity of the second (pulse 2 in Figs 1c, d) has a smaller value. Note that while the peak intensity of the adiabaton probe pulse significantly exceeds the intensity of pulses 1 and 2, the total energy W_1 of the latter is only 2% less than the adiabaton energy even at a distance $s = 800$, which follows from the transmission curves presented in Fig. 2.

Interaction of radiations in the medium leads to a change in the control field characteristics. Its intensity is no longer constant, and the envelope of the field acquires a more complex structure comprising a 'hump' and 'dips' (thin curves in Figs 1b–d). In this case, the hump propagates at a velocity c in front of probe pulses, and each dip resides in the region of one of them. Note that in the case of an adiabaton [30] the curve describing the dependence of the control field intensity on w has a similar hump and a similar dip.

Figure 3 shows the curves describing the dependences of I_1, γ_1 and α_1 on w for several fixed distances s. According to the dependence $\gamma_1(w)$, at a sufficiently small distance ($s = 40$) the leading and trailing edges of the probe pulse become left-handed elliptically polarised ($\gamma \simeq -0.7$), whereas the central part of the pulse remains circularly polarised [curve (*2*) in Fig. 3a]. According to the dependence $\alpha_1(w)$ [curve (*3*) in Fig. 3a] the direction of the major axis of the polarisation ellipse of the leading edge ($\alpha_1 = 0.5$ rad) coincides with the direction of polarisation of the input control field. At the same time, the direction of the major axis of the polarisation ellipse of the trailing edge ($\alpha_1 = 2.07$ rad) is perpendicular to the direction of polarisation of the input control field. With increasing s the degree of ellipticity, i.e. $|\gamma_1|$, decreases and the probe pulse is split into two pulses (Figs 3b, c). At a large distance (Fig. 3d), the probe field is localised in two separate pulses with mutually perpendicular linear ($\gamma_1 = 0$) polarisations, the first pulse being polarised in the same direction as the input control field.

2. Let us now consider EIT in regime II for a strong input probe pulse to compare the results obtained with those of the above calculations. To do this, we set $\tau_1 = 5$, $\alpha_{10} = 0.5$ rad, $a_{10} = 2$, $\gamma_{10} = 0$, $\alpha_{20} = -0.1$ rad, $a_{20} = 4.9$ and $\gamma_{20} = -1$ in (6) and (7). Continuous curves in Fig. 4 show the results of calculations of the dependence of the control and probe field intensities on w for several fixed distances s. Dashed curves show the dependences of the probe pulse intensity in regime III. According to Fig. 4 the input probe pulse in regime II decays

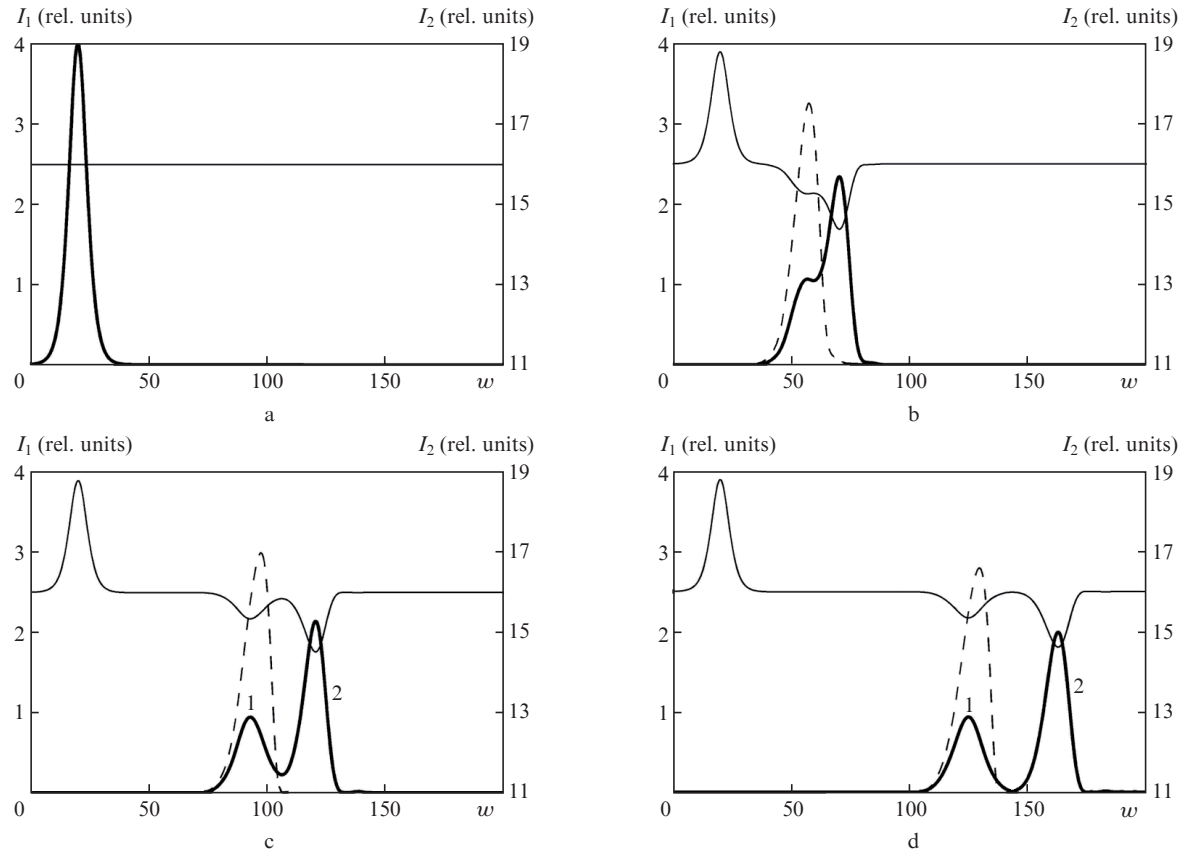

Figure 1. Evolution of I_1 and I_2 in regime I (thick and thin curves, respectively) and of I_1 in regime III (dashed curves) for distances s = (a) 0, (b) 280, (c) 560 and (d) 800.

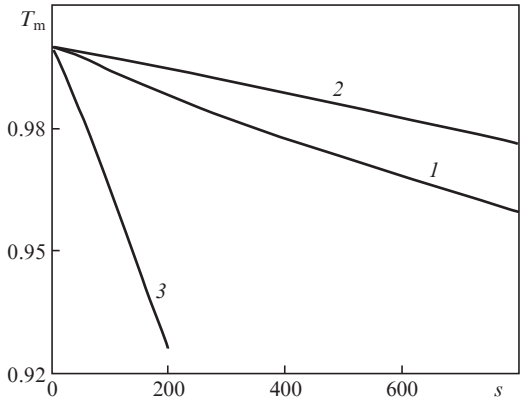

Figure 2. Dependences of the probe pulse transmittance on the distance s for regimes (*1*) I, (*2*) III and (*3*) II.

into three individual pulses in a medium (pulses 1, 2, 3 in Figs 4b–d). The first of them propagates at a velocity that is close to that of an adiabaton probe pulse (dashed curves in Fig. 4), and the other two have lower velocities. This decay occurs at a distance $s < 100$ (Fig. 4c), while the decay of the input probe pulse in regime I requires a much greater distance ($s \approx 800$, Fig. 1d). The shape of the probe field transmission curve in regime II [curve (*3*) in Fig. 2] shows that the process of the splitting of the probe pulse in regime II is accompanied by a somewhat higher energy loss than in regime I.

Apart from the quantitative differences in the results of the numerical analysis for regimes I and II, there is an important qualitative difference in the polarisation states of the probe field pulses, into which the input probe pulse is split in the medium. Figure 5 shows curves describing the dependence of I_1, γ_1 and α_1 on w for two fixed distances s. According to Fig. 5a, near the front surface of the medium the probe pulse begins to decay into subpulses, the first pulse and second pulses having the right- and left-hand elliptical polarisations, respectively (thin curves in Fig. 5a). The directions of the major axes of polarisation ellipses of subpulses coincide with the direction of linear polarisation of the input probe field (dashed curves in Fig. 5a). At a greater distance (s = 80, Fig. 5b), the subpulses are already well separated, with the first of them having σ_- polarisation ($\gamma_1 = 1$), and the second $-\sigma_+$ polarisation ($\gamma_1 = -1$).

3. Let us present the results of calculations for regime I in the case of a weak signal pulse. To do this, we set $\tau_1 = 5$, $\alpha_{10} = -0.1$ rad, $a_{10} = 0.16$, $\gamma_{10} = -1$, $\alpha_{20} = 0.5$ rad, $a_{20} = 7.0$ and $\gamma_{20} = 0$ in (6) and (7). Figures 6a, b show the curves describing the dependence of I_1, γ_1 and α_1 on w for the initial (s = 80) and final (s = 800) stages of the decay of the input probe pulse into linearly polarised components.

Comparison of Figs 6a, b with Fig. 3 shows that the nature of the splitting of the input probe pulse in the medium has not changed: the input probe pulse decays into two subpulses with mutually perpendicular linear polarisations. Moreover, the distance at which the splitting of the input probe pulse occurs is the same in the cases of weak and strong input probe fields.

To illustrate the effect of the input probe pulse duration on its evolution in the medium, we have performed calcula-

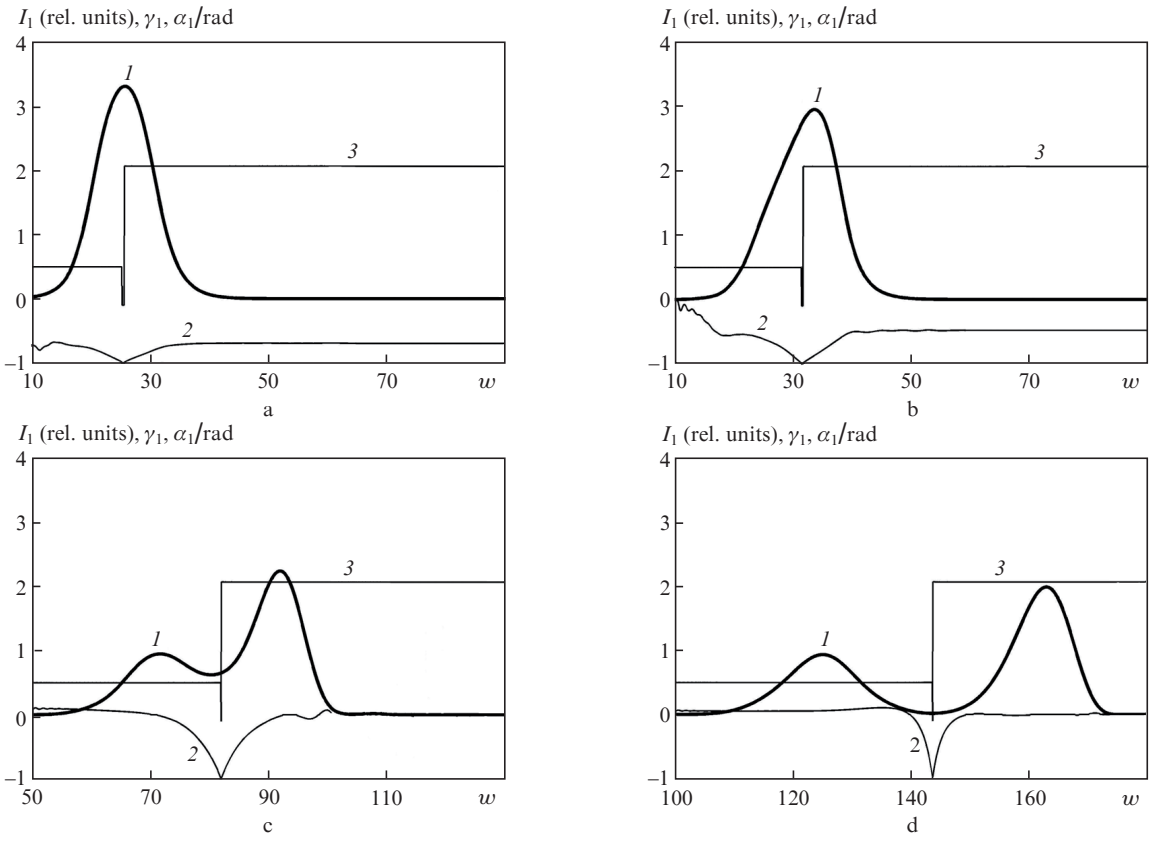

Figure 3. Evolution of (*1*) I_1, (*2*) γ_1 and (*3*) α_1 in regime I for distances s = (a) 40, (b) 80, (c) 400 and (d) 800.

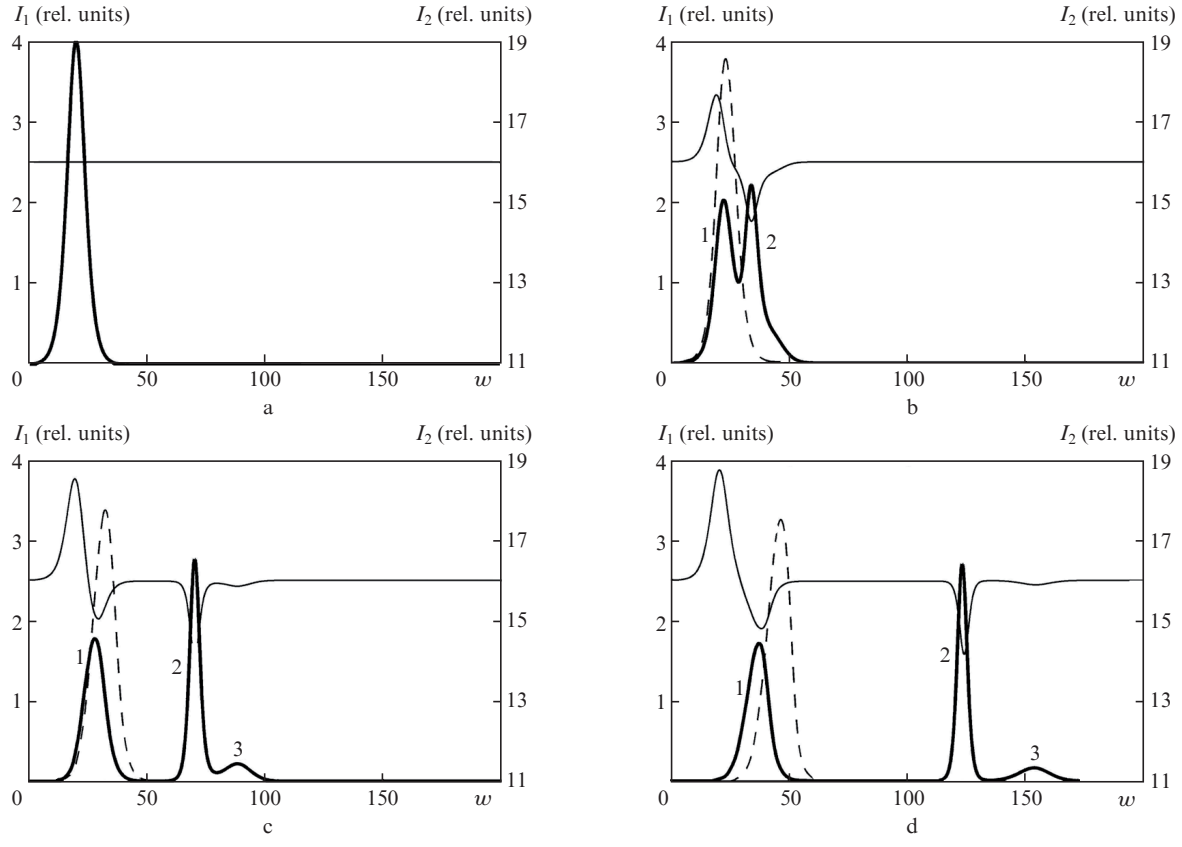

Figure 4. Evolution of I_1 and I_2 in regime II (thick and thin curves, respectively) and of I_1 in regime III (dashed curves) for distances s = (a) 0, (b) 30, (c) 100 and (d) 200.

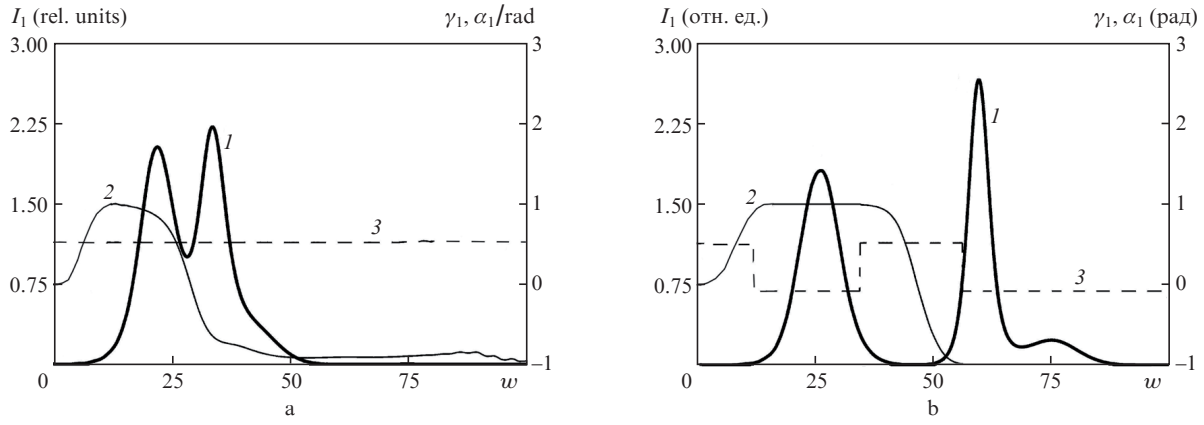

Figure 5. Evolution of (*1*) I_1, (*2*) γ_1 and (*3*) α_1 in regime II for distances s = (a) 30 and (b) 80.

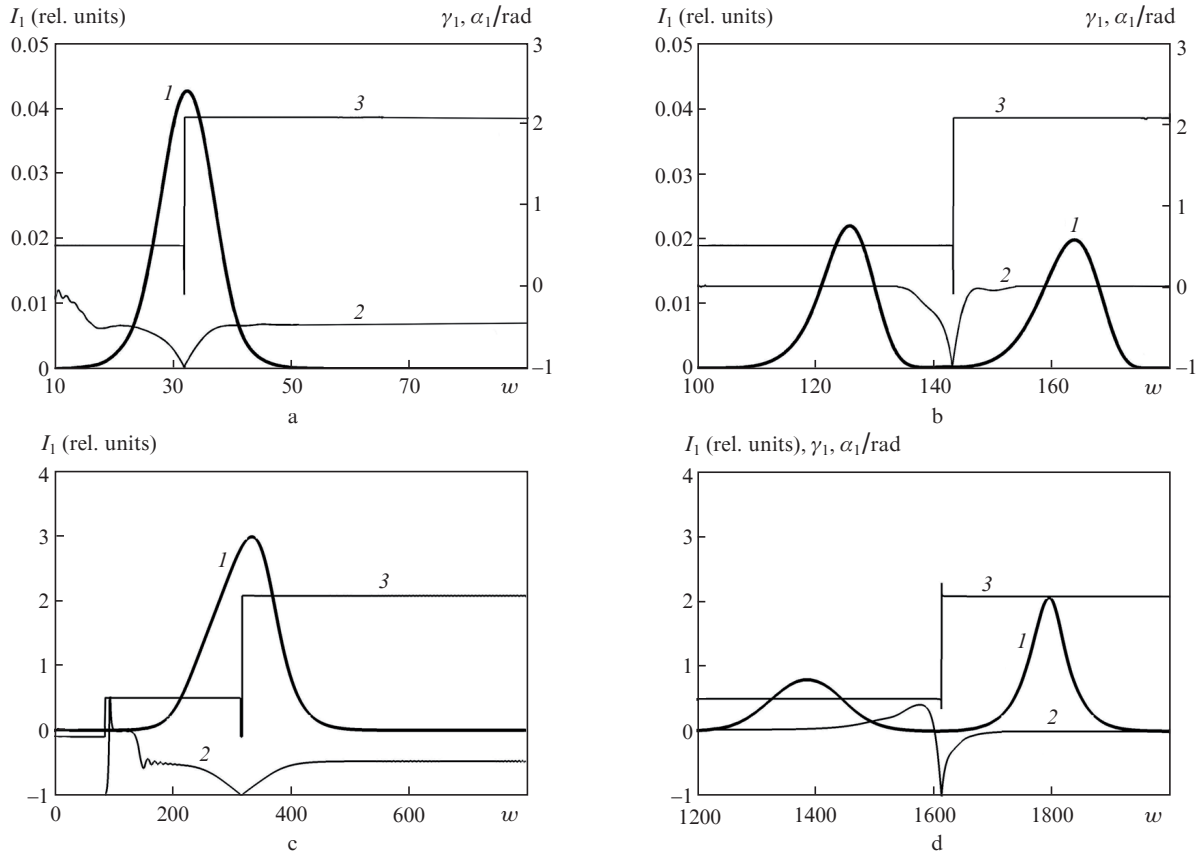

Figure 6. Evolution of (*1*) I_1, (*2*) γ_1 and (*3*) α_1 in regime I for (a, b) a weak input probe pulse and (c, d) a strong input probe pulse at distances s = (a) 80, (b) 800, (c) 810 and (d) 9000.

tions for regime I at a pulse duration $\tau_1 = 50$, i.e. 10 times greater than that used in previous calculations. Figures 6c, d show the curves describing the dependence of I_1, γ_1 and α_1 on w for the initial ($s = 810$) and final ($s = 9000$) stages of the decay of the input probe pulse into linearly polarised components. The curves in Figs 6c, d are also indicative of the splitting of the probe pulse in the medium into two subpulses with mutually perpendicular linear polarisations. However, this splitting takes place at a distance ($s = 9000$) that is approximately 10 times greater than that in the case of a short input pulse.

4. Discussion of the calculation results

Let us present some thoughts on the physical causes leading to the difference in the polarisation properties of the probe field in regimes I and II. Because the analysis of the processes that determine regime II was described in detail in [24, 25], we only briefly recall here its main features. Figure 7a shows the scheme of quantum transitions corresponding to EIT in regime II. Left (right) inclined arrows correspond to quantum transitions induced by $\sigma_+(\sigma_-)$ components of the field. It follows from Fig. 7a that the σ_+ component of the probe field

evolves in the lambda scheme formed by states 1, 4 and 7, and the σ_- component evolves in the lambda scheme formed by states 1, 2 and 5. The moduli of the electric dipole moments of transitions 1–4 and 1–2, resonant with circular components of the probe field, in the lambda schemes in question are identical. At the same time, the moduli of the electric dipole moments of transitions 7–4 and 5–2, resonant with a single circular component of the control field, are different. In this regard, the propagation velocities of σ_+ and σ_- components of the probe field in the medium are also different, and the input probe pulse splits into subpulses circularly polarised in opposite directions.

The decay of the input probe pulse in regime I has a more complex nature. Figure 7b shows the sheme of quantum transitions corresponding to EIT in regime I. In contrast to regime II, here there are two circular components of the control field. The scheme of quantum transitions in Fig. 7b cannot be reduced to two lambda schemes with a common lower level as it was in the case of regime II. Note that the σ_- component of the probe field (dashed line in Fig. 7b) is absent on the input surface. On the other hand, the splitting of the circularly polarised input probe pulse into elliptically or linearly polarised subpulses, detected in the calculations, is not possible without the presence of this component inside the medium.

The formation of the σ_- components of the probe field in the medium takes place for the following reason. According to the equation for the quantity $\partial f_1/\partial s$ in system (4), the source of generation of the σ_- components of the probe field in the medium is the product of $c_1c_2^*$ under the integral sign on the right-hand side of this equation. At $s = 0$ and $w = 0$ and owing to the initial conditions $c_2 = 0$, an excitation source of the σ_- component of the probe field is absent. However, according to the structure of the system of equations (4), at $w > 0$ there appears a chain of quantum transitions between levels 1, 4, 7 and 2 (Fig. 7b) and there occurs the population of state 2. Accordingly, the product $c_1c_2^*$ becomes different from zero, and the σ_- component of the probe field is generated. As the pulse propagates in a medium, the intensity of this component continuously increases. When the intensity of the σ_- components becomes equal to that of the σ_+ component, linearly polarised probe subpulses are formed. After that, both components of the probe pulse propagate in the same conditions, and therefore the equality of their intensities is preserved. Thus, the generation of the σ_- component of the probe pulse involves atoms trapped in the quantum state 2 as a result of the interaction of the waves.

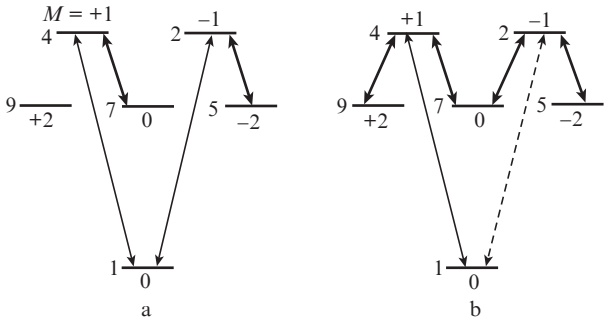

Figure 7. Scheme of quantum transitions in regimes (a) II and (b) I: the numbers to the left of the horizontal lines denote the number of states; the numbers at the top or bottom – the quantum number of the M state; and left (right) inclined arrows show the transitions induced by σ_+ (σ_-) components of the fields.

Figure 8a shows the dependence of the quantity $\rho_{22} = |c_2|^2$, i.e., the population of level 2, on w for three fixed distances s. It can be seen that the maximum population of this level does not exceed 0.05% of the total number of atoms participating in EIT. To this end, a substantial gain of the σ_- component of the probe field requires a fairly long distance. Figure 8b shows the dependences of ρ_{44}, i.e., the population of level 4 directly excited by the σ_+ component of the probe field (Fig. 7b). Because this component is already present at the input surface of the medium, then at a small distance ($s = 8$) $\rho_{44} \gg \rho_{22}$. However, at large distances, when the intensity of circular components of the probe field are comparable, the populations of levels 2 and 4 become approximately equal (Figs 8a, b).

In the case of regime II (Fig. 7a), the intensities of σ_+ and σ_- probe-field components become equal on the input surface of the sample. Both components simultaneously begin to evolve in their lambda schemes. Therefore, the distance at which the input probe pulse decays in regime II is considerably smaller than that in the case of regime I.

Note that as a result of EIT, the input probe pulse in regime I decays in the medium into two pulse with mutually perpendicular linear polarisations. This means that the phase differences of circular components of the probe field are different in various parts, and therefore, the components themselves exhibit phase modulation. This phase modulation is accompanied by many phenomena of resonance [31] and nonresonance [32] optics of short light pulses.

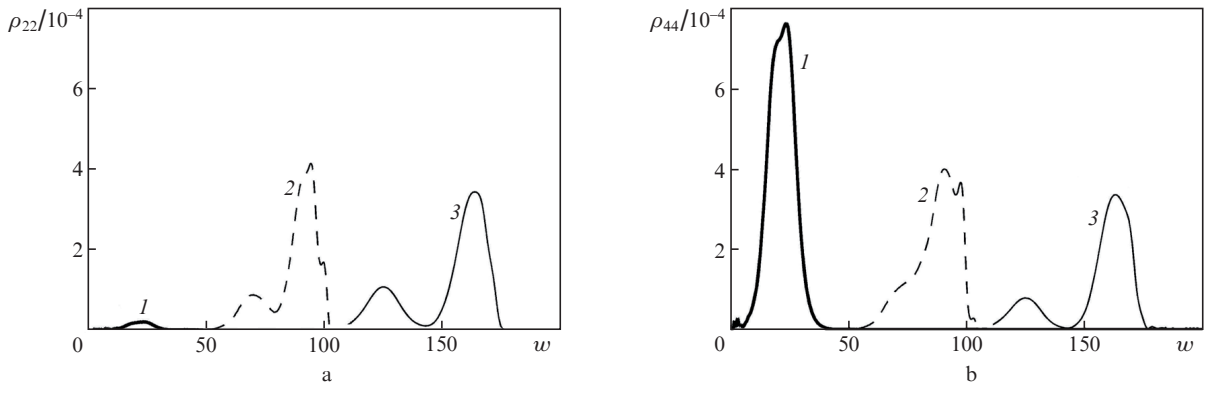

Figure 8. Evolution of the populations of level (a) 2 and (b) 4 for s = (*1*) 8, (*2*) 400 and (*3*) 800.

The splitting of the input probe pulse into subpulses in regimes I and II can be interpreted as the birefringence effects in EIT. In the case of regime I, a circularly polarised input probe pulse is the sum of fields polarised in directions that are collinear and perpendicular to the polarisation direction of the control field. The pulses produced by these components of the probe field propagate with different velocities in regime I, which is manifested as a decay of the input probe pulse inside a medium. (By the pulse velocity is meant the propagation velocity of a point corresponding to its peak intensity in the medium. This value is approximately equal to the rate of the energy transfer by a pulse, if the distortion of the shape of its envelope during the propagation is not too large.) In the case of regime II, the linearly polarised input probe pulse can be given as the sum of the components that are circularly polarised in opposite directions. In a medium these components propagate at different velocities, which leads to the decay of the input probe pulse.

Transient birefringence in EIT has a significant difference from the birefringence effects leading to the electro-optical or optical Kerr effect [33]. The latter is explained by the difference in phase velocities of linearly polarised eigenmodes in a medium with the anisotropy induced by a constant electric field or by an electric field of the optical wave. In the above-described EIT regimes the decay of the input probe pulse is due to the difference in the propagation velocities of pulses with different polarisation states in the medium.

Being a resonant effect, EIT provides a significantly greater efficiency of linear or circular birefringence than that realised in nonresonant processes. Thus, a complete decay of the input probe pulse as a result of EIT in regime I occurs at a distance of 4 cm for $N = 2 \times 10^{14}$ cm^{-3}. Approximately the same distance is usually required to observe the optical Kerr effect in liquids at an almost two orders of magnitude greater intensity of the laser field [34, 35].

5. Conclusions

The results presented demonstrate that EIT on degenerate quantum transitions can be an effective way to implement the specific effect of birefringence that leads to the splitting of the probe pulse into subpulses with different polarisation states. This type of birefringence is significantly different from the previously known types by the fact that it is explained by the difference in the rates of energy transfer by pulses rather than the difference in the phase velocities of light eigenmodes of the medium. Therefore, this birefringence can be called pulsed birefringence. It is linear in the case of linear polarisation of the control field and circular if the field is circularly polarised.

Being resonant, pulsed birefringence is much more effective than the known phenomena of birefringence in nonresonant laser fields. Because pulsed birefringence is a transient effect, it is realised in the case of fairly short pulses of the probe field. The results of the calculations that are not included in this paper show that the change in the intensity of the control field allows one to control the velocities and durations of subpulses arising under pulsed birefringence. The effect of pulsed birefringence may find practical application in the creation of high-speed devices, the functioning of which is associated with the control of polarisation and energy characteristics of laser pulses.

Note that the above-considered scheme of degenerate quantum transitions is relatively simple. One can expect that pulsed birefringence in more complex schemes of quantum transitions used in the study of EIT [5] has specific features that have not been identified in our research.

References

1. Harris S.E. *Phys. Today*, **50**, 36 (1997).
2. Lukin M.D. *Rev. Mod. Phys*., **75**, 457 (2003).
3. Duan L.-M., Lukin M.D., Cirac J.I., Zoller P. *Nature (London)*, **414**, 413 (2001).
4. Sinatra A. *Phys. Rev. Lett*., **97**, 253601 (2006).
5. Fleischhauer M., Imamoğlu A., Marangos J.P. *Rev. Mod. Phys*., **77**, 633 (2005).
6. Martinalli M., Valente P., Failache H., Felinto D., Cruz L.S., Nussenzveig P., Lezama A. *Phys. Rev. A*, **69**, 043809 (2004).
7. Godone A., Micallilizio S., Levi F. *Phys. Rev. A*, **66**, 063807 (2002).
8. Lukin M.D., Imamoğlu A. *Nature (London)*, **413**, 273 (2001).
9. Kocharovskaya O., Mandel P. *Phys. Rev. A*, **42**, 523 (1990).
10. Popov A.K. *Izv. Vyssh. Uchebn. Zaved., Ser. Fiz*., **60**, 99 (1996).
11. Ham B.S., Hemmer P.R., Shahriar M.S. *Opt. Commun*., **144**, 227 (1997).
12. Nikonov D.E., Imamoğlu A., Scully M.O. *Phys. Rev. B*, **59**, 12212 (1999).
13. Abdumalikov A.A. Jr, Astafiev O., Zagoskin A.M., Pashkin Yu.A., Nakamura Y., Tsai J.S. *Phys. Rev. Lett*., **104**, 193601 (2010).
14. Tassin P., Zhang L., Koschny T., Economou E.N., Soukoulis C.M. *Opt. Express*, **17**, 5595 (2009).
15. Cerboneschi E., Arimondo E. *Phys. Rev. A*, **52**, R1823 (1995).
16. MacRae A., Campbell G., Lvovsky A.I. *Opt. Lett.*, **33**, 2659 (2008).
17. Mazets I.E. *Phys. Rev. A*, **71**, 023806 (2005).
18. Wielandy S., Gaeta A.L. *Phys. Rev. Lett.*, **81**, 3359 (1998).
19. Bo Wang, Shujing Li, et al. *Phys. Rev. A*, **73**, 051801(R) (2006).
20. Agarwal G.S., Shubhrangshu Dosgupta. *Phys. Rev. A*, **67**, 023814 (2003).
21. Sautenkov V.A., Rostovtsev Y.V., Chen H., Hsu P., Agarwal G.S., Scully M.O. *Phys. Rev. Lett*., **94**, 233601 (2005).
22. Tai Hyun Yoon, Chang Yong Park, Sung Jong Park. *Phys. Rev. A*, **70**, 061803(R) (2004).
23. Kis Z., Demeter G., Janszky J. *J. Opt. Soc. Am. B*, **30**, 829 (2013).
24. Volkov A.V., Druzhinina N.A., Parshkov O.M. *Kvantovaya Elektron*., **39**, 917 (2009) [*Quantum Electron*., **39**, 917 (2009)].
25. Parshkov O.M. *Kvantovaya Elektron*., **41**, 1010 (2011) [*Quantum Electron*., **41**, 1010 (2011)].
26. Kasapi A., Maneesh Jain, Yin G.Y., Harris S.E. *Phys. Rev. Lett*., **74**, 2447 (1995).
27. Born M., Wolf E. *Principles of Optics* (Oxford: Pergamon Press, 1975; Moscow: Nauka, 1970).
28. DeZafra R.L., Marshall A. *Phys. Rev*., **170**, 28 (1968).
29. Grigoriev I.S., Meilikhov E.Z. (Eds) *Handbook of Physical Quantities* (Boca Raton, NY: CRC Press, 1996; Moscow: Energoatomizdat, 1991).
30. Grobe R., Hioe F.T., Eberly J.H. *Phys. Rev. Lett*., **73**, 3183 (1994).
31. Polouektov I.A., Popov Yu.M., Roitberg V.S. *Kvantovaya Elektron*., **1**, 757 (1974) [*Sov. J. Quantum Electron*., **4**, 423 (1974)].
32. Akhmanov S.A., Vyslouh V.A., Chirkin A.S. *Optics of Femtosecond Laser Pulses* (New York: American Institute of Physics, 1992; Moscow: Nauka, 1988).
33. Shen Y.R. *The Principles of Nonlinear Optics* (New York: John Wiley & Sons, 1984; Moscow: Nauka, 1989).
34. Hellwarth R.W., Owyoung A., George N. *Phys. Rev. A*, **4**, 2342 (1971).
35. Wong G.K.L., Shen Y.R. *Phys. Rev. A*, **10**, 1277 (1974).